Systems & Control Transactions

Research Article - Peer Reviewed Conference Proceeding
ESCAPE 35 - European Symposium on Computer Aided Process Engineering
Ghent, Belgium. 6-9 July 2025
Jan F.M. Van Impe, Grégoire Léonard, Satyajeet S. Bhonsale,
Monika E. Polańska, Filip Logist (Eds.)

PSE PRESS

Environmental Impacts of Trichlorosilane: Process Optimization, Life Cycle Assessment, and the Importance of Processing History

Ethan Errington*[a], Deniz Etit[b], Tom Vinestock[a], Jaewook Lee[a], Jerry Heng[b], and Miao Guo[a]

[a] King's College London, Department of Engineering, London, WC2R 2LS, UK
[b] Imperial College London, Department of Chemical Engineering, London, SW7 2AZ, UK
* Corresponding Author: ethan.errington@kings.ac.uk.

ABSTRACT

Trichlorosilane (TCS) is a platform chemical used in the manufacture of silicon metals, silicones, and functional silanes. Despite this, very little information is available on the environmental impact (EI) associated with its manufacture. This work addresses this gap by developing estimates for the EI of reagent grade TCS (RG-TCS) based on a combination of process modelling & optimisation and life cycle assessment (LCA). Two production methods are considered: 1) direct chlorination (DC) producing RG-TCS as a main product, and 2) the Siemens process (SP) producing RG-TCS as a co-product. Results of a bi-objective process optimization suggest that the DC approach provides consistently better pareto-optimal (PO) trade-offs between the global warming potential (GWP) of RG-TCS and process profit; predicted GWPs are 3.2 to 3.3 $kgCO_2$-eq/kg for DC-derived RG-TCS and 3.8 to 4.9 $kgCO_2$-eq/kg for SP-derived PO designs. This suggests that processing history is important when considering the EI of RG-TCS. Nonetheless, further discussions of model uncertainty stress that these GWP estimates should be considered as preliminary, with improvements to modelling being required to refine EI predictions of RG-TCS in the future.

Keywords: Life Cycle Assessment, Process Modelling, Process Optimization, Trichlorosilane, Silicon

INTRODUCTION

Trichlorosilane (TCS) is a platform chemical used in the manufacture of silicon metals, silicones, and functional silanes. Knowing the environmental impact (EI) of TCS is thus key to understanding the EI of many products, ranging from electronics to adsorbent materials.

Despite the importance of TCS, very little information is available on the environmental impact (EI) of TCS manufacturing. Thus, it is difficult to understand the EI of producing TCS, and TCS-derived products.

One reason for the lack of EI information may be variable production history. For example, reagent grade TCS (RG-TCS, 98wt%) can be produced as a main product of the direct chlorination (DC) of metallurgical grade silicon (MG-Si) [1], or as a co-product of the Siemens process (SP) for high purity silicon metal (≥99.9999 wt%) [2].

While both the DC and the SP rely on the chlorination of MG-Si, they differ in their energy intensity. This suggests the possibility of an importance of processing history in governing the EI of RG-TCS.

One way in which the EI of RG-TCS could be established is through Life Cycle Assessment (LCA). Nonetheless, this would require knowledge of material and energy use associated with gate-to-gate production of RG-TCS. In the absence of real plant data, prior research suggests that process modelling may be the preferred approach for accurately gathering this kind of information [3].

Herein, process modelling-informed LCA models are developed to quantify the EI of RG-TCS with the aim of:

1) detailing typical process designs by which RG-TCS is produced by DC and the SP,
2) identifying pareto optimal (PO) trade-offs in the EI and profitability of DC and the SP designs.
3) establishing the importance of processing history on the EI of RG-TCS products.

This has been done with modelling specific to China given its large share in global SG-Si production [2].

METHODS

Process Description

Direct Chlorination

In the DC method (Figure 1a), hydrogen chloride (HCl) is produced through the reaction of hydrogen (H_2) and chlorine (Cl2) in reactor R1 (Equation 1). HCl is then reacted with MG-Si to produce chlorosilanes in R2 (Equation 2 and 3) [1].

$$H_2 + Cl_2 \rightarrow 2HCl \quad (1)$$

$$3HCl + Si_{MG} \rightarrow SiCl_3H + H_2 \quad (2)$$

$$4HCl + Si_{MG} \rightarrow SiCl_4 + 2H_2 \quad (3)$$

Chlorosilanes in the effluent of R2 are then separated by flash condensation in unit F1 and refined into RG-TCS and silicon tetrachloride (STC, 98wt%) products by distillation in C1 [2]. Residual gases leaving F1 are separated into chlorosilanes and hydrogen in adsorption column (A1) [4]. Recovered hydrogen is recycled and the chlorosilanes are fed to C1 [2].

Siemens Process

The SP (Figure 1b) extends the DC method by further purifying TCS in columns C2 and C3, yielding an RG-TCS product (C2 tops), an ultra-high purity TCS (C3 tops, 99.99 wt%) and residual waste (C3 bottoms) [2]. The TCS from C3 is heated in a furnace (E5) and reduced using hydrogen (3:1 H_2:TCS mole ratio [2]) in reactor R3 to produce solar grade silicon (SG-Si, 99.9999 wt%) according to Equations 4 and 5 [2]. The resulting gases are recycled and STC is hydrogenated to form TCS in R4 [2] (Equation 6); R4 effluent is fed to column C4 for material recovery.

$$SiCl_3H + H_2 \rightarrow Si_{SG} + 3HCl \quad (4)$$

$$2SiCl_3H + HCl \rightarrow SiCl_4 + H_2 \quad (5)$$

$$Si_{MG} + 2H_2 + 3SiCl_4l \rightarrow 4SiCl_3H \quad (6)$$

Process Modelling

Models for the DC and SP methods were built in the Aspen Plus V11 software according to process flow diagrams shown in Figure 1. Vapour-liquid equilibria was modelled using the NRTL-RK method. Equipment with fixed operating conditions are listed in Table 1.

Reaction performance associated with each process was based on patent and academic literature (Table 2). Compressor performance was modelled according to isentropic compression. Distillation was modelled according to the MESH equations.

The production scale of both DC and the SP was based on a 24.1 kmol/hr feed of HCl to reactor R2 [6].

It was assumed that 75% of heat generated by reactors R1 and R2 could be recovered as steam.

Table 1: Thermodynamic information for equipment assumed to have fixed conditions.

Unit	Temperature, C	Pressure, bar	Ref.
R1	250	2.5	[7]
R2	350	5.0	[8]
R3	1100	1.1	[6]
R4	500	36.0	[9]
A1	25	1.1	-
E3	25	1.1	-
E4	25	1.1	-
E5	400	1.1	[6,10]
E6	25	1.1	-
E7	500	1.1	[9]

Table 2: Summary of reaction performance assumed during reaction modelling.

Unit	Equation	Yield, %	Basis (w.r.t)	Ref.
R1	1	100	H_2	[7]
R2	2	^{13}90	Si	[6,10]
	3	^{13}10	Si	[6,10]
R3	4	^{14}30	$SiCl_3H$	[6,12]
	5	^{14}70	$SiCl_3H$	[6,12]
R4	6	^{11}25	$SiCl_4$	[6,8]

Process Optimization

The NSGA-II algorithm [16] (100 individuals, PYMOO package [17]) was used to find PO frontiers for maximisation of the total annualised process profit, TAP ($/yr), and minimization of the Global Warming Potential of RG-TCS (GWP, kgCO_2-eq/kg) for DC and the SP. In each case, optimization was run until a minimum of 4000 profitable designs were found.

$$\min\ [-TAP,\ GWP] \quad (7)$$

$$\text{given: } TAP = f_1(x) \quad (8)$$

$$GWP = f_2(x) \quad (9)$$

$$\text{s.t.: } g(x) \leq 0 \quad (10)$$

$$x^{lb} \leq x \leq x^{ub} \quad (11)$$

Where $g(x)$ is a black-box function based on the underlying process model, Equation 10 represents practical constraints associated with product purity in the black box model, and x^{lb} and x^{lu} represent the lower and upper bounds associated decision vector x. Minimum purities of 98 wt% were set for sale of RG-TCS and STC. A minimum purity of 99.99 wt% TCS was set for the top product of column C3 used to produce SG-Si in the SP method [6].

Process Economics

The TAP of each process was calculated by subtracting the sum of total annualised capital and operational expenditures, TAC and TAO ($/yr), from the total annualised revenue, TAR ($/yr), as shown in Equation 12.

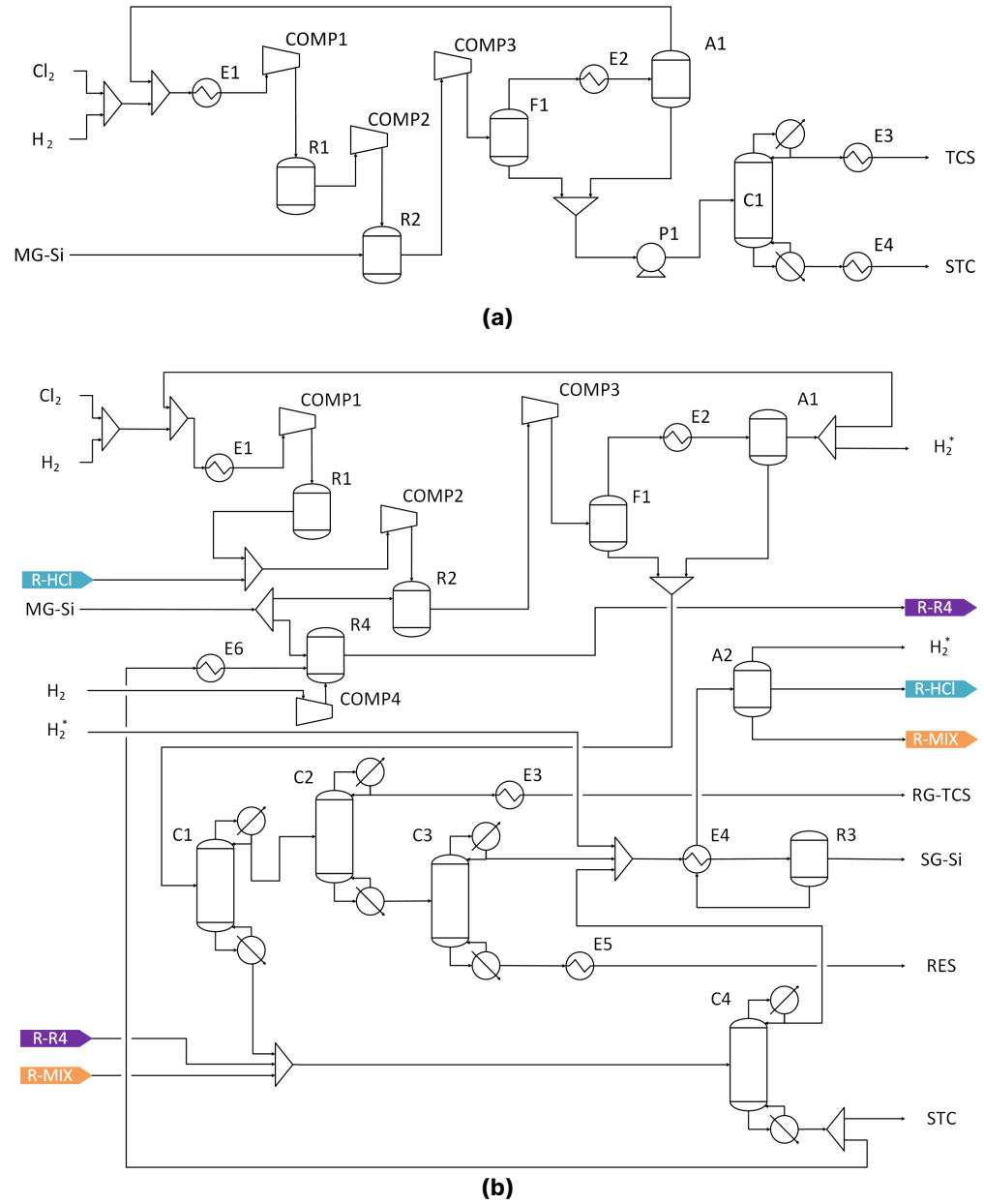

Figure 1: Process flow diagrams for production of trichlorosilane by the direct chlroination (top) and Siemens process (bottom) methods. TCS: trichlorosilane, STC: silicon tetrachloride, RES: residual waste chlorosilanes, MG-Si: metallurgical grade silicon, SG-Si: solar grade silicon, H_2: reagent grade hydrogen; H_2^*: high purity hydrogen.

It was assumed that costs reflected the implementation of a grass-roots plant based on the year 2019.

$$TAP = TAR - (TAC + TAO) \quad (12)$$

Total Annual Revenue

TAR was calculated based on product sales according to Equation 13 and Table 3.

$$TAR = \sum_p P_p \dot{m}_p \quad (13)$$

Where P_p is the sale price of product P_p ($/kg) and $\dot{m}_p$ is the annual production amount of product p ($/kg).

Total Annual Capital Expenditure

TAC was calculated using Equation 14, considering costs associated with compressor, heat exchanger, pump, and distillation units only.

$$TAC = \frac{\sum_e CAPEX_e}{A} \quad (14)$$

Where $CAPEX_e$ is the capital expenditure of unit e ($), and A is an annualization factor (yr) assuming a 30-year payback period and 3% interest rate. $CAPEX$ calculation included bare module costs [15], materials choice [16], and geographic location [16].

Table 3: Assumed material and utility fuel source prices

Material	Price, $/unit	Unit	Ref.
MG-Si	1.75	kg	[18]
Cl_2	0.28	kg	[19]
H_2[a]	0.15/4.00	kg	[19,20]
RG-TCS	1.00	kg	[21]
STC	1.00	kg	[21]
SG-Si	12.00	kg	[18]
Electricity	0.088	kWh	[22]
Coal[b]	4.022	GJ	[22]

[a] prices reflect 98 and 99.99 wt% hydrogen product purities, [b] assuming energy conversion factor of 30 GJ/tonne of coal

Total Annual Operational Expenditure

TAO was calculated including consideration for feedstock use (Table 2), utility use and waste handling (Table 3, as per [17]), and operator labour (as per [15]) according to Equation 15.

$$TAO = \sum P_f \dot{m}_f + \sum P_u \dot{Q}_u + \sum P_w \dot{Q}_w + 4.8 P_{OL} \qquad (15)$$

Where P_f and $\dot{m}_f$ are the price ($/kg) and annual usage (kg/yr) of feedstock f, and P_u and $\dot{Q}_u$ are the price ($/kJ) and annual usage (KJ/yr) of utility, u; P_w and $\dot{Q}_w$ are the price of waste treatment ($/kg) and annual amount of waste produced (kg/yr); and P_{OL} is the price of labor four process operators each with a 36,000 $/yr salary.

Life Cycle Assessment

Goal and Scope Definition

The goal of LCA in this work is to estimate the EI of RG-TCS produced by DC and the SP. An attributional LCA approach was used, considering a cradle-to-gate scope, with 1 kg of RG-TCS as a functional unit.

Inventory Modelling

Life cycle inventories were generated using material and energy use estimates from process modelling & optimization. The EcoInvent Database (v3.10, APOS) [23] was used to model background life cycle activity.

Impact Assessment

The EI of RG-TCS has been estimated using the ReCiPe 2016 (H) method [24] considering the GWP ($kgCO_2$-eq) as a proxy for EI. Calculations include a cut-off factor of 0.1%. Co-product impacts have been allocated according to the mass of product produced.

RESULTS AND DISCUSSION

Results of bi-objective optimization are shown in Figure 2. This data includes three expected trends.

Firstly, results for both processes display a positive correlation between the GWP and profitability of PO process designs for DC and the SP – reflecting the presence of a trade-off between process profit and product GWP.

Secondly, the GWP of SP-derived RG-TCS is observed to be consistently larger than that of DC-derived

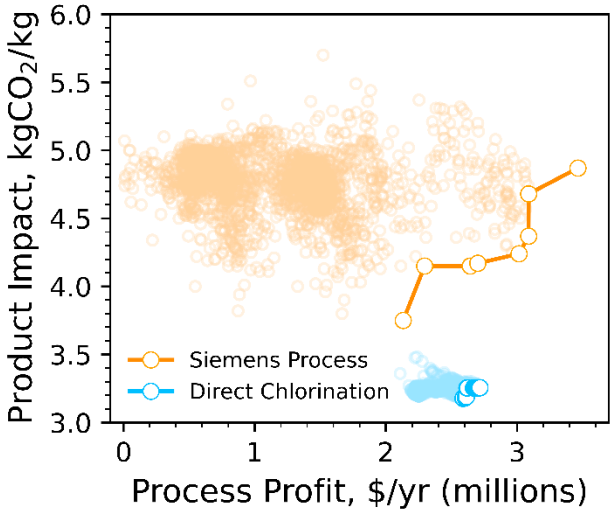

Figure 2: Trade-offs in global warming potential and profitability identified during design optimization. Solid lines outline pareto-optimal designs. Dull markers represent other feasible, non pareto-optimal designs.

RG-TCS for all pareto optimal designs. This is intuitive given the high energy intensity of distillation and production of SG-Si in the SP (see Figure 1).

Thirdly, the PO frontier of DC designs covers a small range of profitability, which may be attributed to the simplicity of DC and lack of competition between reducing EI and maximising profit during design.

On the contrary, Figure 2 also shows two unexpected results.

Firstly, PO designs of the SP cover a very similar range of possible profitability when compared to that of PO DC designs. This is unexpected given the high value of SG-Si produced by the SP method (see Table 3) and complexity of the SP (see Figure 1), which may lead to the expectation of greater return in process profit.

Secondly, the GWP of RG-TCS produced by PO designs of DC and the SP are found to be relatively similar (i.e. 3.2 to 3.3 and 3.8 to 4.9 kg CO_2-eq/kg respectively). This may contradict the expected scale of GWP associated with energy intensity of SG-Si production in the SP.

Relation to Trichlorosilane Yield

To explain unexpected results in Figure 2, further consideration is needed for process designs of PO solutions. Results in Figure 3 illustrate the relationship of RG-TCS yield and process profit for DC and SP designs.

Surprisingly, results for both DC and the SP show designs with high RG-TCS yields (90 to 92 % and 76 to 91 % respectively). This is intuitive for DC designs as the yield of RG-TCS does not compete directly with the yield of STC (see Figure 1), making high yields of RG-TCS likely to reflect materially efficient design implementations.

Conversely, high RG-TCS yields are counterintuitive

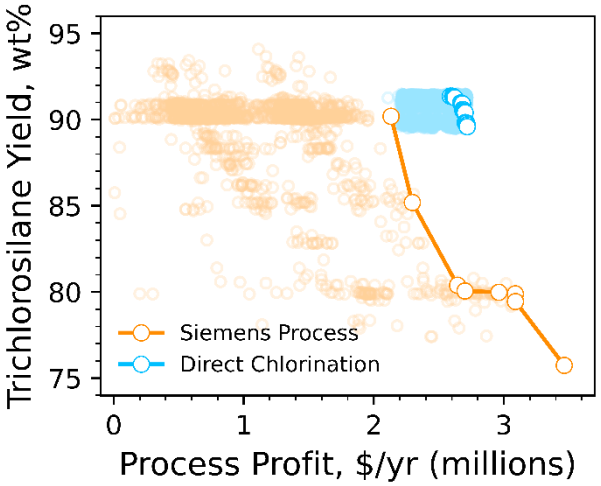

Figure 3: Relationship of trichlorosilane yield and process profit identified during design optimization. Solid lines highlight the location of pareto-optimal designs shown in Figure 2. Dull markers represent other feasible designs.

for the SP - given that the yield of RG-TCS competes directly with the yield of SG-Si (Figure 1). Consequently, the observed PO SP designs must minimise the production of SG-Si - the intended main product of the SP.

To understand why this is, three aspects of the modelling method used must be further considered.

Relation to Impact Allocation Method

One way in which the observed PO SP designs may tend toward maximising RG-TCS yield is through an inherent bias introduced by using a mass-based impact allocation method during LCA. This is because of the relatively high molar mass of TCS (135 g/mol) when compared to Si (28 g/mol), which suggests that the conversion of feedstock to RG-TCS in high yield is likely to minimise the GWP of RG-TCS products by maximising the total mass of products produced by the SP.

Relation to Optimization Algorithm

Another reason why the observed PO SP designs may tend to maximise RG-TCS yield is because of limitations in the optimization algorithm used. Specifically, the optimizer used may have failed to identify regions of the search space in which feasible high-profit, high-impact designs exist - e.g. as a result of maximizing SG-Si yield at the expense of RG-TCS yield and GWP.

This may be corroborated by the fact that multiple high-profit, high-impact SP designs were observed during the early stages of optimization but lost as optimization proceeded due to violating constraints associated with RG-TCS (≥98 wt%). Such designs may have failed to evolve toward feasible solutions due to the use of a strict "feasibility first" constraint handling approach, which prioritises feasible designs over search diversity [17].

Thus, it is possible that the PO frontiers visualised in Figure 3 represent only the low-impact, low-profit subset of the true PO design space available to the SP.

Further research is needed to explore the SP design space more rigorously.

Relation to Process Modelling Uncertainties

Finally, four major sources of uncertainty in process modelling must be considered when interpreting data.

Firstly, the SP modelled (Figure 1) considers only one method for recycling of the chlorosilane-rich effluent which arises after the deposition of SG-Si (see R4, Figure1) [2]. Thus, the reported GWP of SP-derived RG-TCS may not accurately reflect the GWP of RG-TCS produced by SP designs using different material recycling methods.

Secondly, the SP modelled does not consider the possibility of thermally integrating distillation columns. This can cause up to a 50% reduction in energy requirements associated with distillation in the SP [2] – suggesting that reported GWPs may be overestimated in this regard.

Thirdly, the effect of impurities on distillation efficiency has not been modelled. This may cause the GWP to be underestimated due to inaccuracy in material and energy estimates associated with distillation in the SP.

Fourthly, the separation of chlorosilanes, hydrogen and hydrogen chloride via adsorption (see Figure 1) has not been modelled rigorously in this work. This may cause the GWP to be underestimated due to failing to account completely for energy and material efficiency in both DC and SP designs.

CONCLUSIONS

Understanding the environmental impact of trichlorosilane (TCS) is crucial in enabling the impact assessment of many products. Consequently, this work has set out to establish estimates for the impact of reagent grade TCS (RG-TCS) produced according to two approaches - direct chlorination (DC), and the Siemens process (SP) for manufacturing solar-grade silicon (SG-Si).

Using global warming potential (GWP) as a proxy for impact, bi-objective optimization suggests that the impact of SP-derived TCS (3.8 to 4.9 kg CO_2-eq/kg) is larger than that of DC-derived TCS (3.2 to 3.3 kg CO_2-eq/kg). This suggests that the processing history of RG-TCS may be an important factor governing the impact of RG-TCS.

Interestingly, it is also observed that results of the work tend to highlight PO SP designs which prioritise the production of RG-TCS in high yield over SG-Si. This is despite SG-Si being the intended main-product of the SP. This is explained as arising from three main factors affecting modelling and optimization: 1) the use of a mass-basis of impact allocation (which biases PO SP designs to SP designs with high TCS yield), and 2) limitations in the

optimization method used, which has possibly failed to identify PO SP designs of high-impact and high-profit, and 3) uncertainty in process modelling, particularly in the case of modelling designs of the SP.

Consequently, though results suggest that processing history is important in governing the impact of RG-TCS, the absolute value of GWP reported for SP-derived RG-TCS should be considered to be a preliminary estimate with room for future improvement. Findings of the work may be of interest to individuals working to produce chlorosilane materials and TCS-derived products.

ACKNOWLEDGEMENTS

This work has been made possible by funding provided by Scottish Water, the UK EPSRC SSCP Doctoral Training Program, and UKRI Innovate UK. EE also thanks Alex Durkin and Benjamin Lyons of Imperial College London for formative discussions on process systems engineering (inc. process modelling and optimization).

REFERENCES

1. Simmler, W. 2000. Silicon Compounds, Inorganic. In: Ullmann's Encyclopedia of Industrial Chemistry. Wiley-VCH. (2000).
2. Yan D. Siemens Process. In: Handbook of Photovoltaic Silicon. Ed: Yang D. Springer. (2019).
3. Parvatker AG and Eckleman MJ. Comparative evaluation of chemical life cycle inventory generation methods and implications for life cycle assessment results. *ACS Sus. Chem. & Eng.* 7(1):350-367. (2019).
4. Xiqun W, Li T. Pressure swing adsorption system for separation of mixed gas including hydrogen and chlorosilane and/or chlorine hydride. CN Patent 202,620,982U. (2012).
5. Del Coso, G *et al*. Temperature homogeneity of polysilicon rods in a Siemens reactor. *J. Cryst. Growth*. 299(1): 165-170. (2007).
6. Ramírez-Márquez C, *et al*. Process design and intensification for the production of solar grade silicon. *J. of Clean. Prod.* 170: 1579-1593. (2018).
7. Benoit J and Mellard J. Facility and reactor for directly synthesizing hydrochloric acid from hydrogen and chlorine with heat recovery. US Patent No. 9,414,364 B2 (2011).
8. Chee Y and Kunimune T. Hybrid TCS-siemens process equipped with 'turbo charger' FBR; method of saving electricity and equipment cost from TCS-siemens process polysilicon plants of capacity over 10,000 MT/YR. US Patent No. 20,120,114,546 A1. (2010).
9. Erickson CE, and Wagner GS. Hydrogenation of halogenosilanes. U.S. Patent No. 2,595,620. (1952).
10. Diez E, *et al*. Distillation assisted heat pump in a trichlorosilane purification process. *Chem. Eng. Process*. 69: 70-76. (2013).
11. Kotzsch HJ, *et al*. Process for the hydrochlorination of elemental silicon. U.S. Patent No. 4,044,109. (1977).
12. Jain MP *et al*. Studies on hydrochlorination of silicon in a fixed bed reactor. *Ind. Chem. Eng.* 53(2):61-67. (2011).
13. Deb K. *et* al. A fast and elitist multiobjective genetic algorithm: nsga-II. *Trans. Evol. Comp*. 6(2):182–197. (2002).
14. Blank J and Deb K. pymoo: Multi-Objective Optimization in Python. *IEEE Access*. 8: 89497-89509. (2020).
15. van Amsterdam MF. Factorial techniques applied in chemical plant cost estimation: A comparative study based on literature and cases. [Thesis Work]. *TU Delft.* (2018).
16. Sinnott R and Towler G. Chemical Engineering Design. 6th Ed. Elsevier. (2020).
17. Ulrich GD. And Vasudevan PT. Chemical Engineering Process Design and Economics. 2nd Ed. Process Publishing Co. (2004).
18. Jarkin VN, *et al*. Methods of trichlorosilane synthesis for polycrystalline silicon production. Part 2: Hydrochlorination and redistribution. *Modern Elec. Mats.* 7(2): 33-43. (2021).
19. Business Analytiq. https://businessanalytiq.com/. [Accessed 31-Jan-2025]. N.B.: “Hydrogen price index” and “Chlorine price Index”.
20. Global Insight Services. High Purity Hydrogen
21. Alibaba. https://www.alibaba.com/. [Accessed 31-Jan-2025]. N.B.: “Trichlorosilane” and “tetrachlorosilane”. Market Analysis and Forecast to 2034. (2025).
22. Statista. https://www.statista.com. [Accessed 31-Jan-2025]. N.B.: “Business electricity price china “ and “South china coal price”.
23. Wernet, G *et al*. The ecoinvent database version 3 (part I): overview and methodology. *Int. J. of LCA*. 21(9): 1218–1230. (2016).
24. Huijbregts, MAJ, *et al*. ReCiPe 2016: a harmonized life cycle impact assessment method at midpoint and endpoint level report I: characterization. (2016).https://rivm.openrepository.com/